International Journal of Coal Geology 197 (2018) 20–30

Contents lists available at ScienceDirect

International Journal of Coal Geology

journal homepage: www.elsevier.com/locate/coal

Responses of specific surface area and micro- and mesopore characteristics of shale and coal to heating at elevated hydrostatic and lithostatic pressures

M. Mastalerz[a,d], L. Wei[b,c,*], A. Drobniak[a], A. Schimmelmann[d], J. Schieber[d]

[a] Indiana Geological and Water Survey, Indiana University, 611 N. Walnut Grove Ave., Bloomington, IN 47405, USA
[b] School of Energy resource, China University of Geosciences (Beijing), Beijing 100083, China
[c] Key laboratory of marine reservoir evolution and hydrocarbon enrichment mechanism, Ministry of Education, Beijing 100083, China
[d] Department of Earth and Atmospheric Sciences, Indiana University, 1001 E. 10th St., Bloomington, IN 47405-1405, USA

ARTICLE INFO

Keywords:
Shale
Coal
Thermal maturity
Porosity
Temperature
Pressure

ABSTRACT

Samples of the low-maturity New Albany Shale (Middle and Upper Devonian to Lower Mississippian) and Mowry Shale (Late Cretaceous), both containing kerogen Type II, and samples of Wilcox Coal (Eocene), containing kerogen Type III, were heated to 60, 100, and 200 °C at hydrostatic ambient pressure, 100, or 300 MPa for 6 or 12 months in sealed glass and gold cells to investigate temperature and pressure effects on porosity and thermal maturity. In addition, lithostatic experiments were conducted in a hydraulic press at 100 MPa and 100 °C over a period of 6 months. Porosimetric characteristics of samples before and after experiments were investigated by using low-pressure gas adsorption and scanning electron microscope (SEM).

An increase from ambient temperature to 200 °C caused increases in random vitrinite reflectance (R_o) for all samples, with Mowry Shale showing the largest increase from 0.57% to 0.65% and Wilcox Coal showing the smallest increase from 0.39% to 0.41%. For Mowry Shale and New Albany Shale, specific surface areas did not change in any notable way with an increase in temperature; specific surface area values for Mowry Shale ranged from 2.0 to 3.2 m^2/g, and for New Albany Shale from 13.7 to 15.6 m^2/g. Differences in Barrett-Joyner-Halenda (BJH) specific mesopore volumes and average mesopore size for the shales were also small to negligible. Considering the values of the original samples, we propose that these small differences are related to internal inhomogeneity of samples rather than to any temperature effect. Temperature-related changes in Wilcox Coal were more distinct. Specifically, there was a marked decrease in BET surface area, from 4.9 m^2/g at 60 °C to 1.5 m^2/g at 200 °C, and a decrease in both BJH mesopore volume and average mesopore size. The Wilcox Coal sample had large micropore surface areas (110–148 m^2/g) compared to both shales, which had micropore surface areas below 10 m^2/g. While Wilcox Coal showed a drop in micropore volume between 60 °C and 200 °C, no distinct or regular changes in micropore volume with temperature were documented for the other two samples.

A sustained hydrostatic pressure increase from ambient to 300 MPa for 6 to 12 months resulted in insignificant changes in vitrinite reflectance values. Small differences in Brunauer-Emmett-Teller (BET) specific surface areas, micropore surface area, and volume may be related to internal sample heterogeneity rather than pressure treatment. Similar to the temperature effect, the Wilcox Coal sample experienced more pronounced changes compared to the shales. SEM observations on shales did not reveal porosity-related changes between the original and treated samples. No marked changes were documented for lithostatic pressure conditions at 100 MPa and 100 °C. We conclude that elevated isotropic hydrostatic or lithostatic pressure is unable to significantly affect the pore structure and pore-size distribution of shales, but it can make some modifications in the micropore and mesopore pore characteristics of low-rank coal.

1. Introduction

The effects of temperature and pressure on the thermal maturity of organic matter have been widely discussed both for natural and experimental conditions. It is well accepted that temperature plays the dominant role, as demonstrated for areas that experienced regional thermal maturation (e.g., Stadler and Teichmüller, 1971; Hower and Gayer, 2002), short-term contact thermal maturation (e.g., Kisch and

* Corresponding author at: Indiana Geological and Water Survey, Indiana University, 611 N. Walnut Grove Ave., Bloomington, IN 47405, USA.
E-mail address: linwei@indiana.edu (L. Wei).

https://doi.org/10.1016/j.coal.2018.06.026
Received 7 March 2018; Received in revised form 29 May 2018; Accepted 21 June 2018
Available online 21 July 2018
0166-5162/

Taylor, 1966; Mastalerz and Jones, 1988; Quaderer et al., 2016), and simulated maturation in laboratory experiments (e.g., Huang, 1996). In turn, there are conflicting opinions about the influence of pressure. It is well demonstrated that effective stress promotes physical changes but generally is thought to retard chemical reactions during thermal maturation (Huck and Patteisky, 1964; Bostick, 1973; Carr, 1999; Carr, 2000; Day-Stirrat et al., 2012).

Effective stress-related physical changes are most important during sediment consolidation and early sediment compaction, resulting in the decrease of total porosity (e.g., Day-Stirrat et al., 2012). Afterwards, with an increase in thermal maturation, hydrostatic and lithostatic pressures are thought not to promote but rather retard temperature-related chemical reactions (e.g., Huck and Patteisky, 1964; Bostick, 1973). Dalla Torre et al. (1997), conducting experiments over pressure range of 0.5 (50 MPa) to 20 kbar (2000 MPa) at temperatures of 200 to 350 °C showed that increasing pressure resulted in suppression of vitrinite reflectance. Other researchers emphasized that increasing static fluid pressure is a major controlling factor in organic matter thermal maturation, and high hydrostatic pressure has been implicated to cause retardation of organic matter maturation (Price and Wenger, 1992; Zou and Peng, 2001). Other laboratory experiments suggested that shear stress and strain could promote structural changes, causing ordering of organic matter and ultimately leading to graphitization (Taylor, 1971; Mastalerz et al., 1993; Wilks et al., 1993; Bustin et al., 1995).

While the influence of temperature and pressure on the thermal maturity of coal and shale has been studied extensively and frequently discussed in the literature, their impact on porosity and pore-size distribution during diagenesis is not well understood. It has been well documented that clay-rich sediments experience large volume loss with an increase in effective stress. Dewhurst et al. (1998) in their experimental studies of compaction effects on weakly consolidated mudstones having 43 to 48% porosity exposed to 33 MPa effective stress documented a decrease in total porosity but no change in the specific surface area. They suggested that pores with pore throats smaller than 20 nm in radius were essentially responsible for all surface area, and pores with throats smaller than 4 nm contributed > 50% of the total surface area. They also documented a decrease in the modal pore throat size from 30 nm to 15 nm in radius between 2 and 33 MPa for a clay-rich sample, whereas in a silt-rich sample, original trimodal pore throat-size distribution (with peaks at ~5–6 μm, 700–800 nm, and 6 nm in radius) transformed to unimodal distribution, resulting in the disappearance of the modes centered at 5 to 6 μm and 700 to 800 nm at 33 MPa. Yang and Aplin (1998) also documented decreases in porosity of mudstones from 27 to 12% with an increase in effective stress from 16 to 28 MPa, because of the collapse of pores larger than 15 nm. Day-Stirrat et al. (2012), studying mudstones to ~600 m below the sea floor, documented a decrease in total porosity with depth from about 80% at the sea floor to 37% at 612 m below the sea floor. In their study, the decrease in total porosity was accompanied by a shift in the pore-size distribution toward smaller pores. Specifically, a reduction in porosity from 49 to 37% caused a loss of pores > 110 nm in radius and the creation of pores having pore throats between 10 and 110 nm in radius. A further decrease in total porosity to 31% resulted in a further reduction of pore sizes to < 70 nm.

In all those studies, the original mudstones were weakly consolidated, had high porosities, and even after exposure to high pressure, their porosities were still relatively high, higher than in mature shales in sedimentary basins. The purpose of this study is to investigate experimentally if elevated temperature and high pressure modify surface area and micropore (pore size < 2 nm) and mesopore (pore size 2–50 nm) characteristics in low-porosity shales and coal, and if so, whether these modifications are similar to those in high porosity clay-rich sediments undergoing compaction or, in other words, if there is a disconnect between thermally immature mudrocks and well consolidated mudrocks of higher maturity. Our investigation utilized high experimental pressures of up to 300 MPa that are rarely associated with economically important shales and coals, yet extreme experimental conditions are necessary to arrive at measurable responses in rocks from laboratory experiments that cannot be extended over geologic time.

Table 1
Characteristics of the samples used in experiments.

Rock unit name	Stratigraphic Age	Location	TOC (wt%)	Random R_o (%)	Total porosity (%)
Mowry Shale	Cretaceous	Colorado	2.5	0.57	8
New Albany Shale	Devonian	Indiana	1.2	0.42	9
Wilcox Coal	Paleocene	Texas	58.0	0.39	23
Springfield Coal	Carboniferous	Indiana	72.0	0.51	15

2. Materials and methods

This study used low-maturity Mowry and New Albany Shales and Wilcox Coal having random vitrinite reflectance (R_o) values ranging from 0.39 to 0.57% and various total organic carbon (TOC) contents (Table 1). Springfield Coal (R_o 0.51%) was used only in lithostatic experiments to substitute for Wilcox Coal. Porosimetric properties of original samples were determined using helium porosimetry (total porosity), low-pressure N_2 adsorption (surface area and mesopore characteristics), low-pressure CO_2 adsorption (micropore characteristics), and mercury intrusion capillary pressure (MICP, for pore throat analysis). Our classification of micropores (< 2 nm diameter), mesopores (2–50 nm diameter), and macropores (> 50 nm diameter) follows that of the International Union of Pure and Applied Chemistry (Orr, 1977). Details about porosimetry techniques can be found in Mastalerz et al. (2013).

Experimental details of heating coal and shale samples in sealed glass or gold cells at various temperatures and hydrostatic pressures are presented in Wei et al. (2018). In brief, rocks were crushed to 1 to 3 mm chip-size fractions, evacuated at room temperature for 2 days, and flooded with nitrogen gas to limit the amount of oxygen in pore spaces. For experiments at ambient pressure, 0.5- to 1-g aliquots of rock chips were sealed together with 0.5 mL of water in 9-mm glass tubes under vacuum. The internal pressure was regulated by steam partial pressure and gas production. For high-pressure experiments, 0.5- to 1-g aliquots of rock chips were placed with water in 6-mm o.d. gold tubes. After sealing the gold tubes with an argon arc welder, we loaded them into pressure containers that were hydrostatically pressured to 100 or 300 MPa (i.e., depth equivalent of ~5 to 15 km). Combinations of pressures (ambient, 100, 300 MPa) and temperatures (ambient, 60, 100, 200 °C) were used in experiments lasting from 6 to 12 months (Wei et al., 2014). The conditions for the samples selected for this study are listed in Tables 2, 3, and 4. The final temperature was achieved within a few minutes and the sample remained at this temperature for the entire experiment duration.

At the end of each heating period, the glass tubes and gold cells were retrieved and connected to the evacuated inlet system of a glass vacuum line to extract and collect gas that had been liberated during experiments (Gao et al., 2014). Solid residues from the experiments were analyzed for vitrinite reflectance and low-pressure gas adsorption porosimetry. A Leica DM 25000 P Microscope with a TIDAS PMT IV attachment was used to collect reflectance measurements, whereas ASAP2020 porosimeter was used to perform low-pressure adsorption analysis. In addition, SEM imaging was performed on select samples to visualize pore distributions.

In addition to hydrostatic pressure experiments, to compare the influence of hydrostatic versus lithostatic pressure, splits of Mowry Shale and New Albany Shale were heated at 100 °C for 6 months at a

Table 2
Changes in random vitrinite reflectance (R_o), BET specific surface area (sa), and mesopore and micropore characteristics with increases in temperature. BET = Brunauer-Emmett-Teller; BJH = Barrett-Joyner-Halenda; D-R = Dubinin-Radushkevich; D-A = Dubinin-Astakhov.

		N_2 adsorption			CO_2 adsorption		
T (°C)	R_o (%)*	BET sa (m^2/g)	BJH meso vol (cm^3/g)	Average mesopore size (nm)	D-R micro sa (m^2/g)	D-A micro volume (cm^3/g)	Average micropore size (nm)
Mowry Shale [ambient pressure]							
Original	0.57	2.7	0.0104	16.1	7.5	0.0057	0.8
60	0.57	2.4	0.0106	18.0	8.3	0.0102	1.1
100	0.63	2.0	0.0105	22.0	12.5	0.0034	0.9
200	0.65	3.2	0.0132	17.0	7.7	0.0087	1.3
New Albany Shale [100 MPa]							
Original	0.42	14.7	0.0243	7.2	7.7	0.0098	1.4
60	0.41	13.7	0.0241	7.9	8.9	0.0176	1.3
100	0.43	14.6	0.0249	7.5	7.9	0.0137	1.4
200	0.44	15.6	0.0272	7.5	8.6	0.0166	1.3
Wilcox Coal [ambient pressure]							
Original	0.39	3.0	0.0148	20.8	140.4	0.0572	1.5
60	0.39	4.9	0.0167	23.1	148.2	0.0630	1.5
200	0.41	1.5	0.0061	17.5	110.2	0.0484	1.4

Note: R_o represents average values of at least 25 measurements with standard deviation below 0.02 for all samples.

lithostatic pressure of 100 MPa. Because of a shortage of Wilcox Coal, Springfield Coal was used in these experiments. A Carver hydraulic press 3851–9 was used for the lithostatic experiments. For these experiments, approximately 2 g of moist sample chips were wrapped in lead foil, and magnesium oxide was used as an external fluid pressure medium. Moist samples were used to avoid artificial fracturing caused by increased pressure.

3. Results

3.1. Original samples

Three low-maturity samples used in experiments with elevated hydrostatic pressures (Table 1), including New Albany Shale and Mowry Shale (containing kerogen Type II) and Wilcox Coal (kerogen Type III) ranged in TOC content from 1.2 wt% in New Albany Shale to 58 wt% in Wilcox Coal. In addition, Springfield Coal, having 72 wt% TOC, was employed in experiments using elevated lithostatic pressure. The total porosity of samples ranged from 8 to 23% (Table 1). Gas adsorption and MICP porosimetric data demonstrate that the total pore volume is $^{<}0.05\ cm^3/g$ for the shales and $\sim 2\ cm^3/g$ for Wilcox Coal (Fig. 1A, B). MICP data indicate that mesopores (2–50 nm diameter) are dominant in the shales (Fig. 2A, B), whereas macropores (> 50 nm diameter) dominate in coal; Fig. 2C. Because MICP cannot access pores $^{<}3$ nm, no micropores (< 2 nm diameter) are reported by this technique. In turn, low-temperature gas adsorption suggests that micropore volumes account for approximately 20% of the total pore volumes of all samples (Fig. 1A).

Pore-throat-radius distributions (Fig. 2) are drastically different among shales and coal. The Wilcox Coal sample had the largest fraction of mercury (Hg) intruded into macropore throats ranging from 100 to 1000 nm in radius (Fig. 2C), whereas the shales expressed a distinct maximum of Hg intrusion into (i) mesopore throats slightly above 10 nm radius for New Albany Shale (Fig. 2B), and (ii) dominantly into $^{<}8$ nm pore throats in Mowry Shale (Fig. 2A). Pore throats of macropore size ($^{>}50$ nm diameter, $^{>}25$ nm radius) are clearly rare in the shales, which agrees with other studies, including those on New Albany Shale (Mastalerz et al., 2013), whereas the prominence of macropore-sized throats in the Wilcox Coal sample supports the general macroporous nature of low-rank coals (e.g., Gan et al., 1972).

The three samples studied differ greatly regarding their Hg injectivity. Wilcox Coal had > 50% Hg injected before the pressure reached 6.9 MPa (1000 psi), whereas a 50% Hg saturation required 68.9 MPa (10,000 psi) for New Albany Shale and an even much higher pressure for Mowry Shale (Fig. 3). These differences are due to contrasting pore size, pore connectivity, and permeability, with Wilcox Coal having the largest pores and permeability and Mowry Shale being

Table 3
Changes in random vitrinite reflectance (R_o), BET specific surface area (sa), and mesopore and micropore characteristics with increasing hydrostatic pressure. BET = Brunauer-Emmett-Teller; BJH = Barrett-Joyner-Halenda; D-R = Dubinin- Radushkevich; D-A = Dubinin-Astakhov.

				N_2 adsorption			CO_2 adsorption		
P (MPa)	Time (months)	T (°C)	R_o (%)*	BET sa (m^2/g)	BJH mesopore volume (cm^3/g)	Average mesopore size (nm)	D-R micropore surface area (m^2/g)	D-A micropore volume (cm^3/g)	Average micropore size (nm)
Mowry Shale									
Original		20	0.57	2.7	0.0104	16.1	7.5	0.0057	0.8
0.1	6	60	0.57	2.4	0.0106	18.0	8.3	0.0102	1.1
100	6	60	0.58	2.6	0.0125	19.5	5.1	0.0201	0.7
300	6	60	0.59	2.7	0.0123	18.8	8.8	0.0098	1.3
New Albany Shale									
Original		20	0.42	14.7	0.0243	7.2	7.7	0.0098	1.4
0.1	6	60	0.42	13.5	0.0248	7.9	10.0	0.0227	1.3
100	6	60	0.41	13.7	0.0241	7.6	8.9	0.0176	1.3
300	6	100	0.42	14.6	0.0248	7.4	7.5	0.0125	1.4
0.1	6	200	0.49	15.3	0.0274	7.8	8.0	0.0145	1.3
100	6	200	0.44	15.6	0.0272	7.5	8.6	0.0166	1.3
300	6	200	0.45	15.6	0.0281	7.7	8.3	0.0138	1.3
Wilcox Coal									
Original		20	0.39	3.0	0.0148	20.8	140.4	0.0572	1.5
0.1	6	60	0.39	4.9	0.0167	23.1	148.2	0.0630	1.5
100	12	60	0.41	3.8	0.0192	20.9	145.9	0.0606	1.5
0.1	6	200	0.41	1.5	0.0061	17.5	110.2	0.0484	1.4
100	6	200	0.41	3.2	0.0168	22.1	120.5	0.0500	1.4

Note: R_o represents average values of at least 25 measurements with standard deviation below 0.02 for all samples.

Table 4
The effect of 100 MPa lithostatic pressure and 100 °C over 6 month period. Comparison of random vitrinite reflectance (R_o), specific BET surface area (sa), and mesopore and micropore characteristics between original and pressurized samples. BET = Brunauer-Emmett-Teller; BJH = Barrett-Joyner-Halenda; D-R = Dubinin-Radushkevich; D-A = Dubinin-Astakhov.

		N_2 adsorption			CO_2 adsorption		
T (°C)	R_o (%)*	BET surface area (m^2/g)	BJH mesopore volume (cm^3/g)	Average mesopore size (nm)	D-R micropore surface area (m^2/g)	D-A micropore volume (cm^3/g)	Average micropore size (nm)
Mowry Shale [100 MPa]							
Original	0.57	6.6	0.0212	13.4	8.6	0.0065	1.4
100	0.59	5.6	0.0175	12.7	7.6	0.0074	1.4
New Albany Shale [100 MPa]							
Original	0.58	6.6	0.0190	11.7	11.7	0.0105	1.2
100	0.6	11.4	0.0256	9.4	9.7	0.0082	1.3
Springfield Coal [100 MPa]							
Original	0.51	9.2	0.0174	8.2	98.8	0.0467	1.4
100	0.51	8.8	0.0143	7.0	100.6	0.0418	1.4

Note: R_o represents average values of at least 25 measurements with standard deviation below 0.02 for all samples.

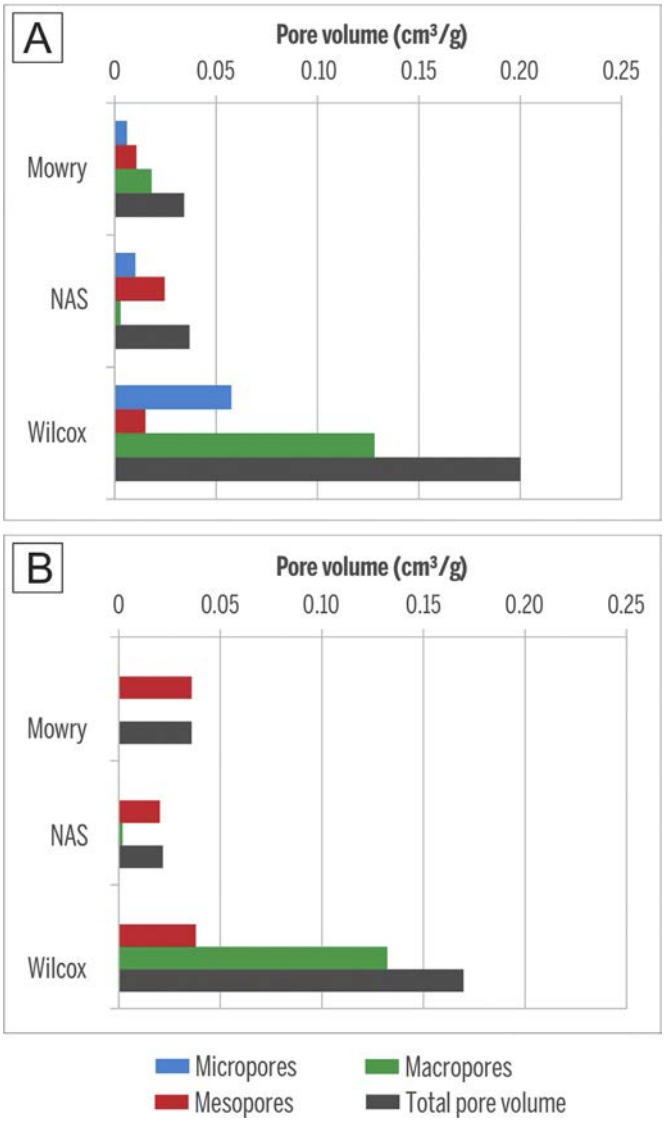

Fig. 1. Pore volumes of original samples as determined by gas adsorption (A) and MICP (B). NAS – New Albany Shale.

the tightest of all three samples and likely having abundant closed pores (Fig. 2).

3.2. Temperature effect

An increase in temperature from room temperature to 200 °C increased R_o most strongly for Mowry Shale (from 0.57 to 0.65%), less for New Albany Shale (from 0.41 to 0.44%), and the least for Wilcox Coal (from 0.39 to 0.41%) (Table 2, Fig. 4A).

For the shale samples, BET specific surface areas did not change notably after heating and stayed within 2.0 to 3.2 m^2/g for Mowry Shale, which is close to the values of the original samples (Table 2, Fig. 4B). In comparison, New Albany Shale has a significantly larger specific surface area (possibly because of mineralogical differences) ranging from 13.7 m^2/g at 60 °C to 15.6 m^2/g after heating to 200 °C at a pressure of 100 MPa (Table 2). The slight increase in specific surface area in New Albany Shale in heating from 60 to 200 °C is likely related to internal inhomogeneity rather than thermal maturation when we consider the even larger specific surface area of 14.7 m^2/g of the unheated original New Albany Shale. The only notable change was recorded for Wilcox Coal—a decrease in BET specific surface area at 200 °C to 1.5 m^2/g from 3 cm^2/g in the original sample.

BJH mesopore volume data mirror the changes observed for specific surface areas where values for New Albany Shale top those of other samples (Table 2). Considering possible internal sample heterogeneity, we did not detect significant changes during heating to 60 and 100 °C, although at 200 °C both shales express increased mesopore volumes, while Wilcox Coal drastically lost mesopores (Table 2). After heating to 200 °C, the average size of mesopores was like that in the original sample for New Albany Shale (7.5 nm versus 7.2 nm), but decreased in Mowry Shale and Wilcox Coal.

Wilcox Coal exhibits a large micropore surface area of 110 to 148 m^2/g compared to $^{<}10$ m^2/g for the shales (Table 2). Upon heating, the New Albany Shale micropore surface area maintained a narrow range of 7.7 to 8.9 m^2/g, whereas Mowry Shale's micropore surface area first increased at 100 °C and later decreased at 200 °C. In contrast, Wilcox Coal's micropore surface area dramatically decreased between 60 and 200 °C. There is no information for Wilcox Coal at 100 °C because the sample was lost during experiment. While Wilcox Coal showed a large drop in micropore volume between 60 and 200 °C, no distinct parallel changes in micropore volume were documented for the shales (Fig. 4C).

3.3. Pressure effect in hydrostatic conditions

Experiments at elevated hydrostatic pressures up to 300 MPa for 6

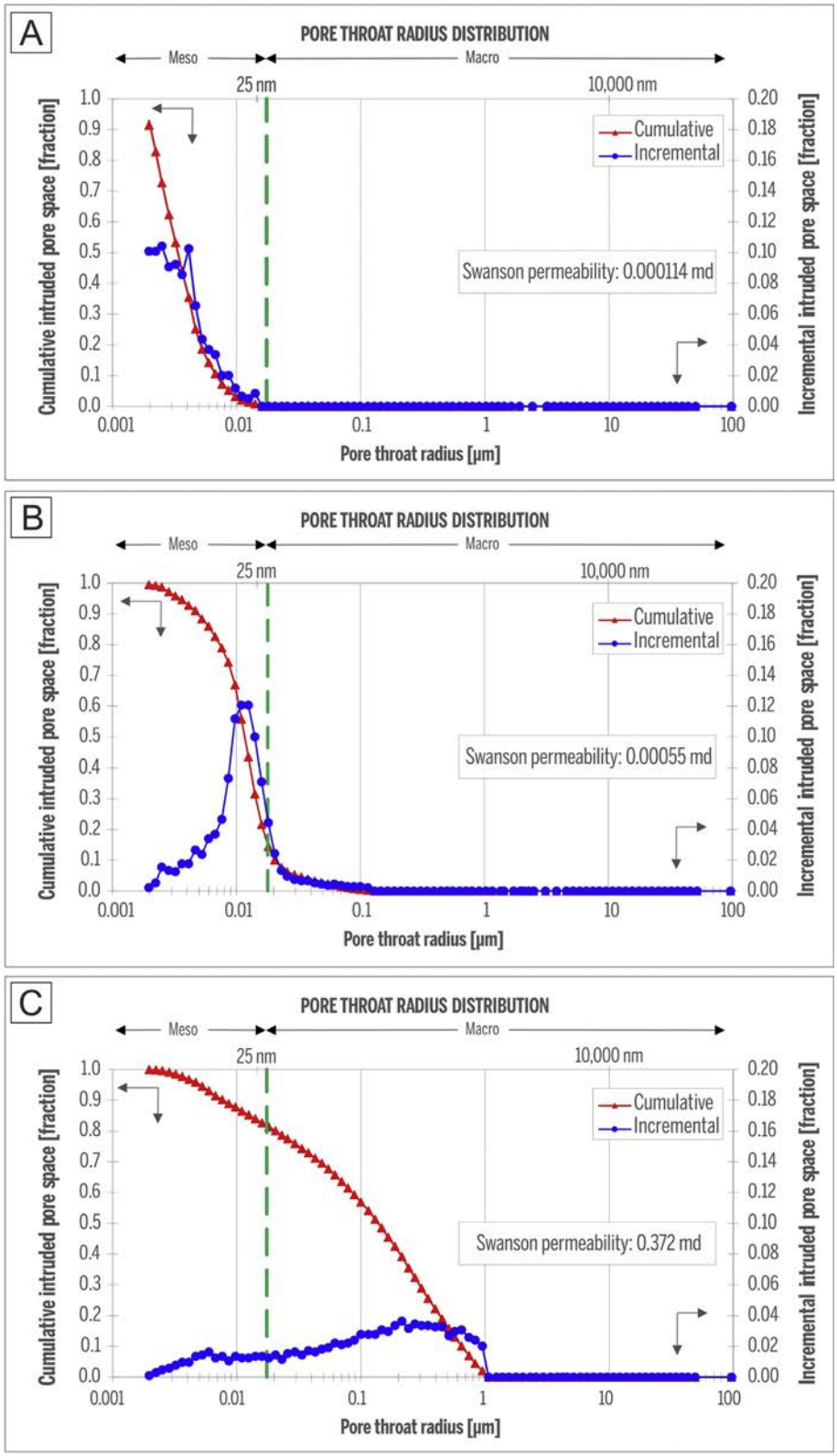

Fig. 2. Graphs showing MICP-derived pore-throat-size distributions of the samples used in experiments: (A) Mowry Shale; (B) New Albany Shale, and (C) Wilcox Coal.

to 12 months caused insignificant changes in (i) vitrinite reflectance within the precision of R_o measurements (Table 3, Fig. 5), and (ii) in BET specific surface areas, which may have resulted from the internal inhomogeneity of samples (Fig. 5A). Inhomogeneity is suspected specifically for Wilcox Coal; the difference of 1.9 m^2/g in BET specific surface area was observed between the original coal and the sample after heating to 60 °C at ambient pressure (3.0 versus 4.9 m^2/g; Table 3). New Albany Shale may have been more susceptible to hydrostatic pressure because its BET specific surface area increased from 13.5 m^2/g (60 °C, ambient pressure) over 13.7 m^2/g (60 °C, 100 MPa) to

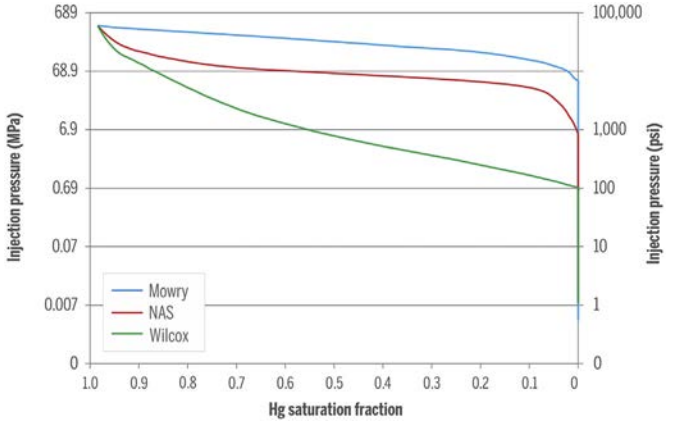

Fig. 3. Mercury (Hg) saturation curves for samples of Mowry Shale, New Albany Shale, and Wilcox Lignite. The contact angle between mercury and pore is 130 °C, and the injection pressure ranges from ambient to 413 MPa.

14.6 m^2/g (100 °C, 300 MPa). However, BET specific surface areas of New Albany Shale after heating to 200 °C are similar in experiments using different hydrostatic pressures, testifying against the influence of the pressure alone. (See Fig. 5.)

Like the specific surface areas, the BJH mesopore volumes of the shales express limited sensitivity to pressure during experiments. In contrast, the BJH mesopore volume in Wilcox Coal increases during heating at 60 °C and even more dramatically at 200 °C (Table 3, Fig. 5B). No trend in average mesopore size with pressure has been revealed for any sample (Table 3). Similarly, there is no clear pressure effect on micropore surface and micropore volume (Table 3, Fig. 5C), where the observed small changes could easily be related to sample inhomogeneity, as suggested by values for original untreated samples.

3.4. Pressure effect in lithostatic conditions

Comparing micro- and mesopore characteristics of original and lithostatically pressurized samples (Table 4) shows a marked difference only for the New Albany Shale under pressure in terms of (i) increased BET specific surface area and mesopore volume, and (ii) decreased micropore volume. Mowry Shale and Springfield Coal did not show notable changes in mesopore or micropore characteristics.

3.5. SEM observations

Comparative SEM observations were carried out on New Albany Shale samples before and after experiments. SEM imaging identified phyllosilicate framework (PF) pores as the dominant pore type, where pores usually occur as triangular openings defined by platelets of clay minerals (Fig. 6A–D). Pores vary in size from several nanometers to several micrometers and can be open or filled with organic matter. Carbonates typically contain dissolution pores with irregular shapes and uneven corroded grain margins. Intragranular dissolution pores are less frequently observed within carbonate grains. Other types of intragranular pores were found in pyrite framboids and rarely in organic matter.

A comparison of SEM images of New Albany Shale samples that were either (i) untreated, (ii) heated to 200 °C for 6 months at ambient pressure, or (iii) heated to 200 °C for 6 months at 300 MPa hydrostatic pressure revealed no obvious differences in terms of pore types or size (Fig. 6E–H). PF pores in the original samples look like those in the samples heated to 200 °C at ambient pressure and at 300 MPa hydrostatic pressure. Although no pores were visible in New Albany Shale organic matter after heating at ambient pressure, some pores were observed after experiments at 300 MPa hydrostatic pressure. The finding of some organic pores in the original untreated samples suggests that any absence of such pores in select samples was due to internal heterogeneity.

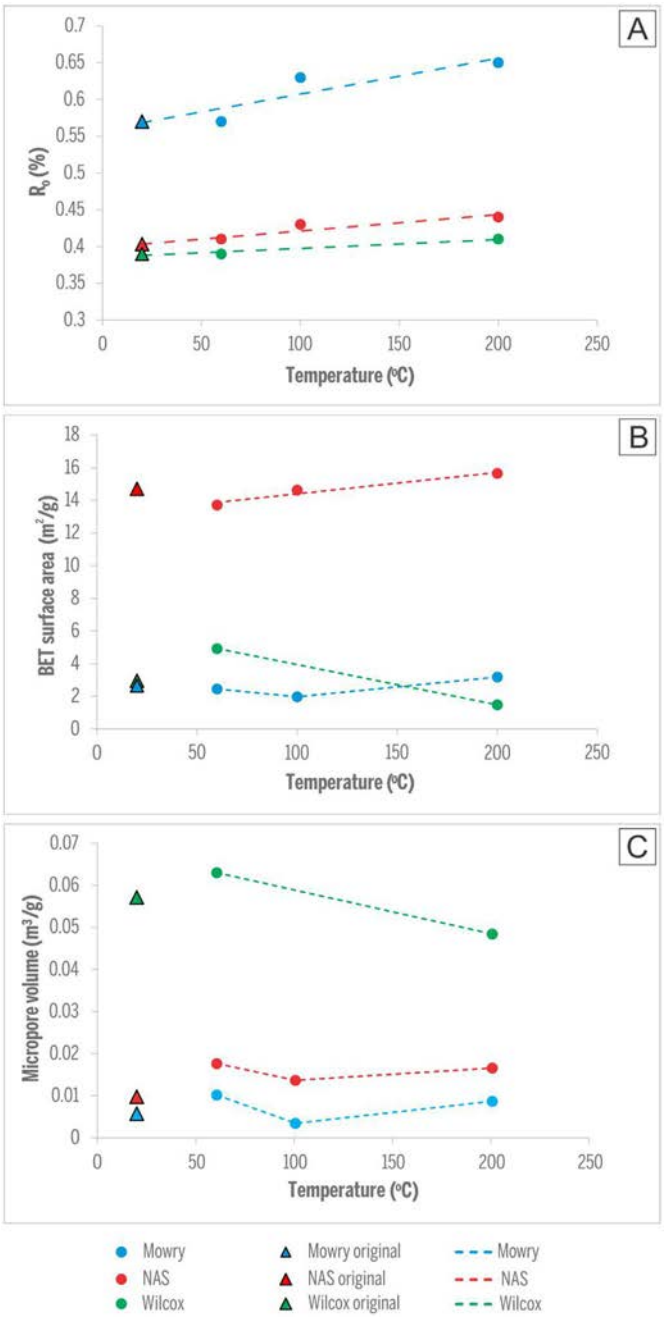

Fig. 4. Temperature effect on (A) random vitrinite reflectance, (B) BET specific surface area, and (C) D–A micropore volume of Wilcox Coal, Mowry Shale, and New Albany Shale.

4. Discussion

While there are well-defined changes in total porosity and pore-size distribution during early compaction of porous sediments at low maturity (Dewhurst et al., 1998; Yang and Aplin, 1998; Day-Stirrat et al., 2012), changes in porosity-related characteristics during advanced diagenesis of fine-grained sediments are more difficult to predict. This study provides insights about the parameters that are less susceptible to changes versus the porosity-related modifications that can be expected in low-porosity shales and coal with increasing temperature and effective stress (Fig. 7).

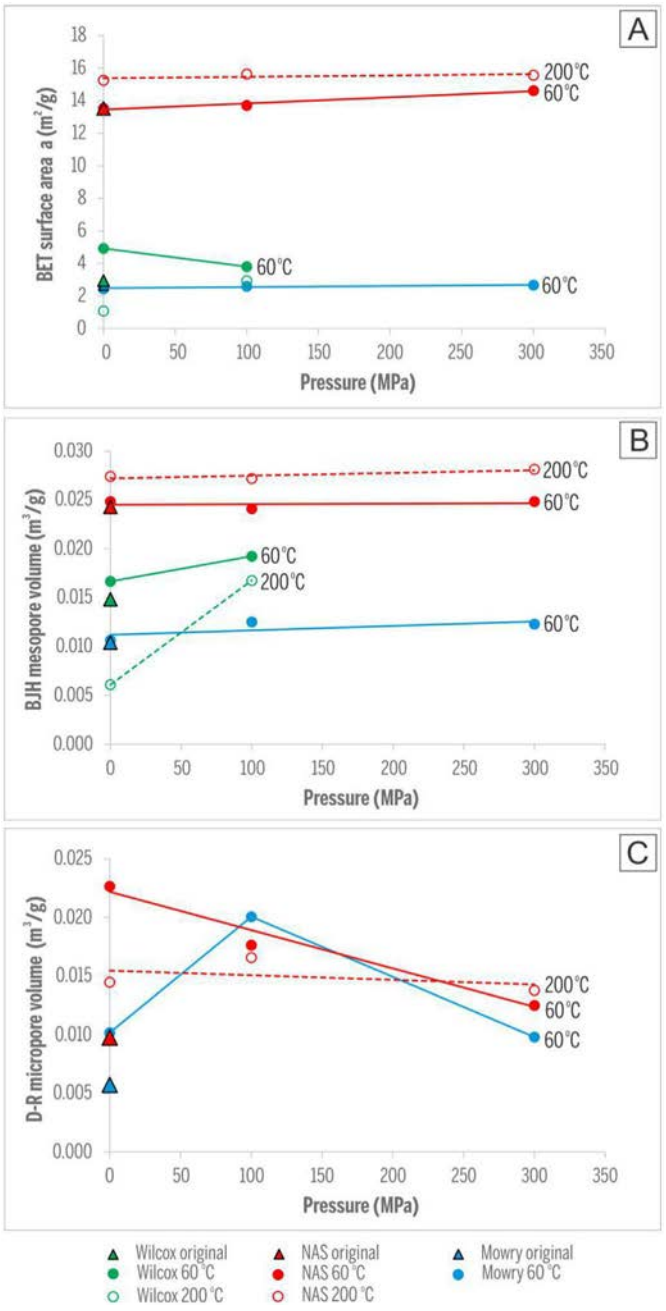

Fig. 5. Hydrostatic pressure effect on (A) BET specific surface area, (B) BJH mesopore volume, and (C) D–A micropore volume of Wilcox Coal, Mowry Shale, and New Albany Shale.

In this study, the temperatures used in the experiment are low (room temperature, 60, 100, and 200 °C), lower than in most laboratory experiments; however, they were selected to be comparable to the temperature regime in many natural systems. We note that for the original samples used in this study, the maximum temperature during thermal maturation assessed from vitrinite reflectance (Barker and Pawlewicz, 1994) was ~60 °C for Wilcox Coal, ~65 °C for New Albany Shale, and ~80 to 90 °C for Mowry Shale. As such, an experimental temperature of 60 °C was not expected to make any modifications of thermal maturity. Indeed, only temperatures of 100 °C and 200 °C (higher than thermal maturation temperatures) caused increases in thermal maturity during the 6 months of the duration of the experiment (Table 2). This increase in thermal maturity is very small, however; it is much smaller than that experienced, for example, by organic matter around intrusions. Around the intrusive dike, Quaderer et al. (2016) show that Springfield Coal experienced an increase in vitrinite reflectance from 0.65% at ~100 °C to ~1.5% at 200 °C. In that study, approximately 100 °C was the regional coalification temperature of that coal. Although that study showed that clastic sediments associated with the coal recorded a lower increase in reflectance compared to the coal (specifically, marine shale above the coal increased its vitrinite reflectance from the original 0.55% to ~0.70% at 100 °C, and to ~1.3% at 200 °C), those thermal maturity increases are still much more prominent that in our study for a similar temperature range and not much different thermal maturity of the original samples. This very modest increase in vitrinite reflectance may be related to the retardation effect of pressures as high as 100 and 300 MPa. We also note that the combined effects of temperature and pressure caused by volcanic intrusions into coal caused significant decreases in surface areas and micropore volumes in Springfield Coal (Mastalerz et al., 2009), in contrast to very limited changes of this study.

The main objective of our study was to explore the modification of mesopore and micropore systems as a result of increasing temperature and pressure. For coal, it has been well documented that the pore structure changes with increasing coalification and micropore volume increase relative to volumes of macropores and mesopores (e.g., Gan et al., 1972; Clarkson and Bustin, 1996). For the samples studied, however, there is only a minimal increase in thermal maturation, and therefore no significant changes were expected because of this small increase.

The only notable temperature-related changes are decreasing specific surface area, mesopore volume, and micropore volume between 60 °C and 200 °C for Wilcox Coal (Table 2; Figs. 4, 7). For the shales, small and irregular differences could be explained by internal heterogeneity of the samples, as suggested by the porosimetric differences between the original samples and those at 60 °C. The original sample of Wilcox Coal was characterized by a much larger pore volume than the shales (Fig. 1); both macropores (> 50 nm in diameter) and micropores (< 2 nm) and the more pronounced temperature effect suggest that abundant organic matter pores experienced temperature-related shrinkage. Changes in much less abundant organic pores in shales were likely not large enough to influence overall surface areas and meso- and micropore volumes. We note that large decreases in surface areas and micropore volumes were documented where Springfield Coal was close to a volcanic dike (Mastalerz et al., 2009), clearly an effect of high temperature.

Changes in mesopores and micropores with increasing pressure were of special interest in this study because 1) pressure has been known to affect the physical properties of rocks, and low-maturity organic matter should be especially susceptible to such changes; and 2) some changes in porosity characteristics in coals and shales are being explained as pressure effects. For example, Mastalerz et al. (2008) analyzed mesopore and micropore characteristics of the Pennsylvanian Seelyville Coal Member from the Illinois Basin and suggested that an increase in the depth of burial and corresponding hydrostatic pressure could reduce surface areas and mesopore volume of the coal, but less so in terms of micropore volume. Our study using a hydrostatic pressure range from ambient to 300 MPa did not reveal any notable changes in mesopores or micropores for shale samples. No changes in macropores for shales were revealed by SEM either. The only notable change was an increase in BET surface area, mesopore volume, and micropore surface area for Wilcox Coal (Table 3, Fig. 7). Based on experimental studies of weakly consolidated sediments, it has been demonstrated that the dominant porosity loss in mud occurs through the collapse of larger pores (> 15 nm), with smaller pores being rather unaffected (Dewhurst et al., 1998; Yang and Aplin, 1998). As shown by gas adsorption and MICP measurements of the samples in this study, Wilcox Coal had highest contribution of large pores (> 100 nm in diameter); perhaps shrinkage of macropores into mesopores caused the increase in the mesopore volume of the coal (Fig. 5B). This suggestion is consistent

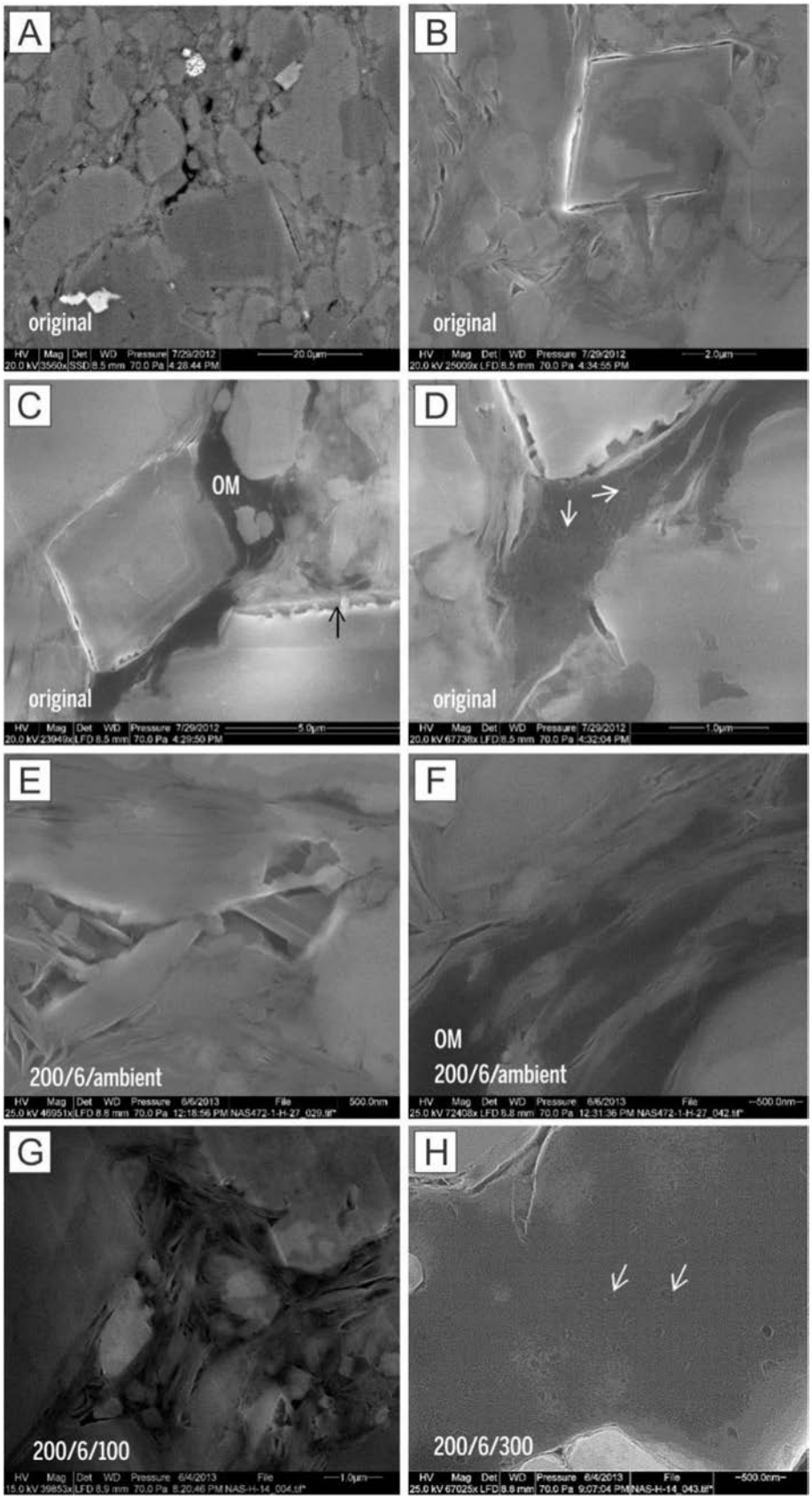

Fig. 6. (A–D) SEM images of the original untreated New Albany Shale samples, and (E–H) of treated New Albany Shale samples. (A) typical view; (B) dolomite rhomb surrounded by cracks that may be related to clay dehydration or dissolution of dolomite; small phyllosilicate framework (PF) pores are also present; (C) dolomite crystals with dissolution pores and organic matter (OM) along grain boundaries; organic matter appears nonporous; (D) close-up of (C) where pores in organic matter become visible; (E) PF pores, 200 °C, 6 months, ambient pressure; (F) organic matter devoid of pores, 200 °C, 6 months, ambient pressure; (G) PF pores and subhorizontal expansion cracks, 200 °C, 6 months, 100 MPa; (H) pores in organic matter, 200 °C, 6 months, 300 MPa.

with the large increase in all ranges of pores of 2 to 100 nm in diameter (Fig. 8A), likely because of shrinkage of macropores larger than 100 nm. The pores of the 2- to 5-nm-diameter range experienced the relatively largest increase at 100 MPa compared to Wilcox Coal at ambient pressure. It has been further suggested that pores smaller than 100 nm in diameter are generally stronger and more resistant to

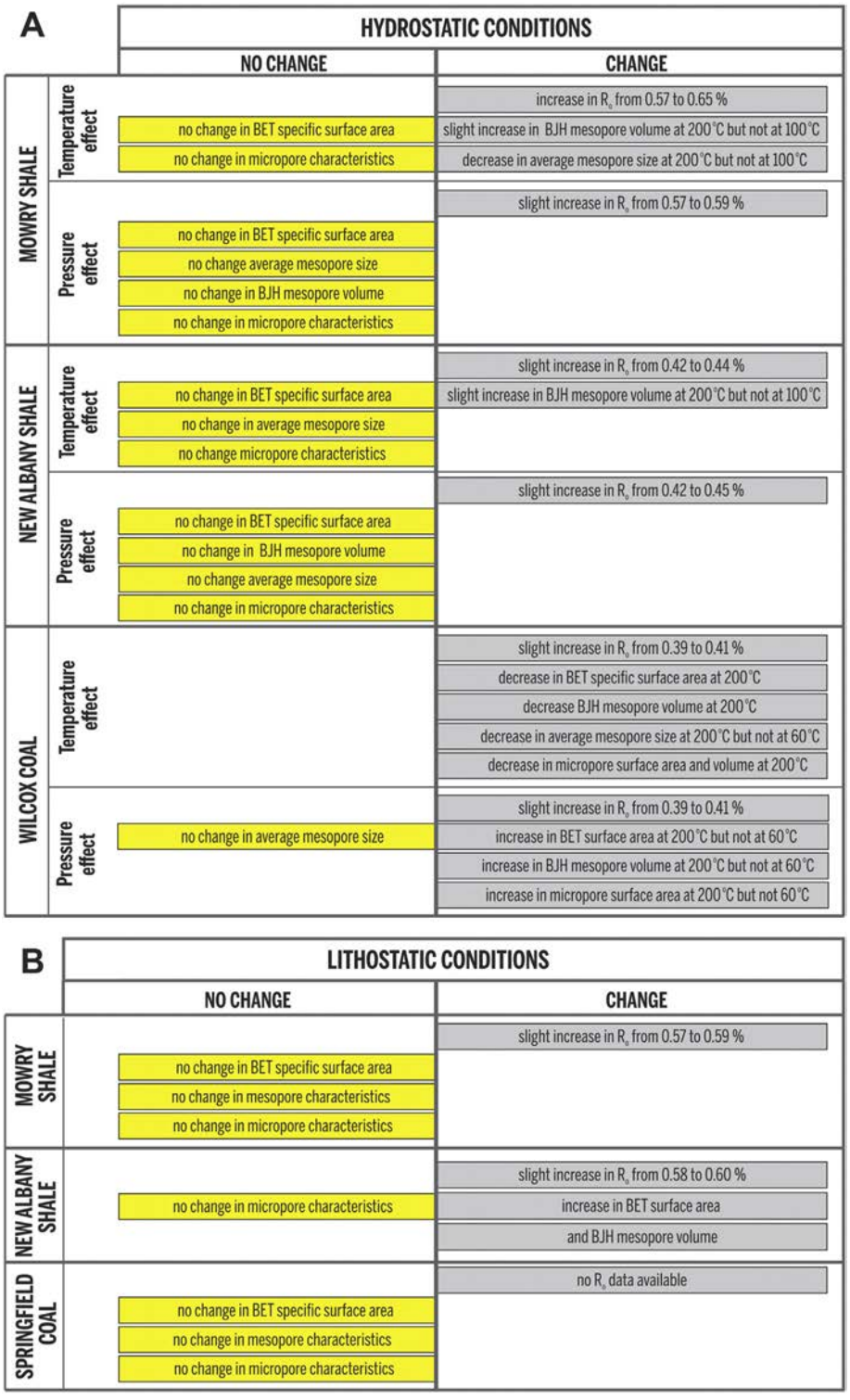

Fig. 7. Temperature and pressure effects on the porosimetry and thermal maturity of the samples studied. (A) Hydrostatic conditions; (B) Lithostatic conditions.

mechanical compaction than larger pores (Loucks et al., 2009; Milliken and Curtis, 2016).

In our samples, pores larger than 100 nm were present in significant quantities only in Wilcox Coal (Fig. 2C), but the stronger nature of smaller pores is consistent with minimal to no change in pore volumes of 2 to 100 nm range in the shales (Fig. 8B). No change in the surface area of the shale samples also suggests that if there were any changes in pore volume, it would have had to be for the largest existing pores. It has been documented experimentally that specific surface area is independent of effective stress up to at least several tens of MPa (Vasseur et al., 1995; Dewhurst et al., 1998), because most of the surface area is contributed by very small pores that are not affected by effective stress. Therefore, even though total porosity may decrease, any expected decrease in surface area is compensated by the larger pores shrinking to a smaller size and a consequent decrease in pore sizes (e.g., Day-Stirrat et al., 2012). For our Wilcox coal sample, surface areas increased significantly for pores throughout the 2 to 100 nm range at 100 MPa, with the highest increase recorded for the 28 to 100 nm range

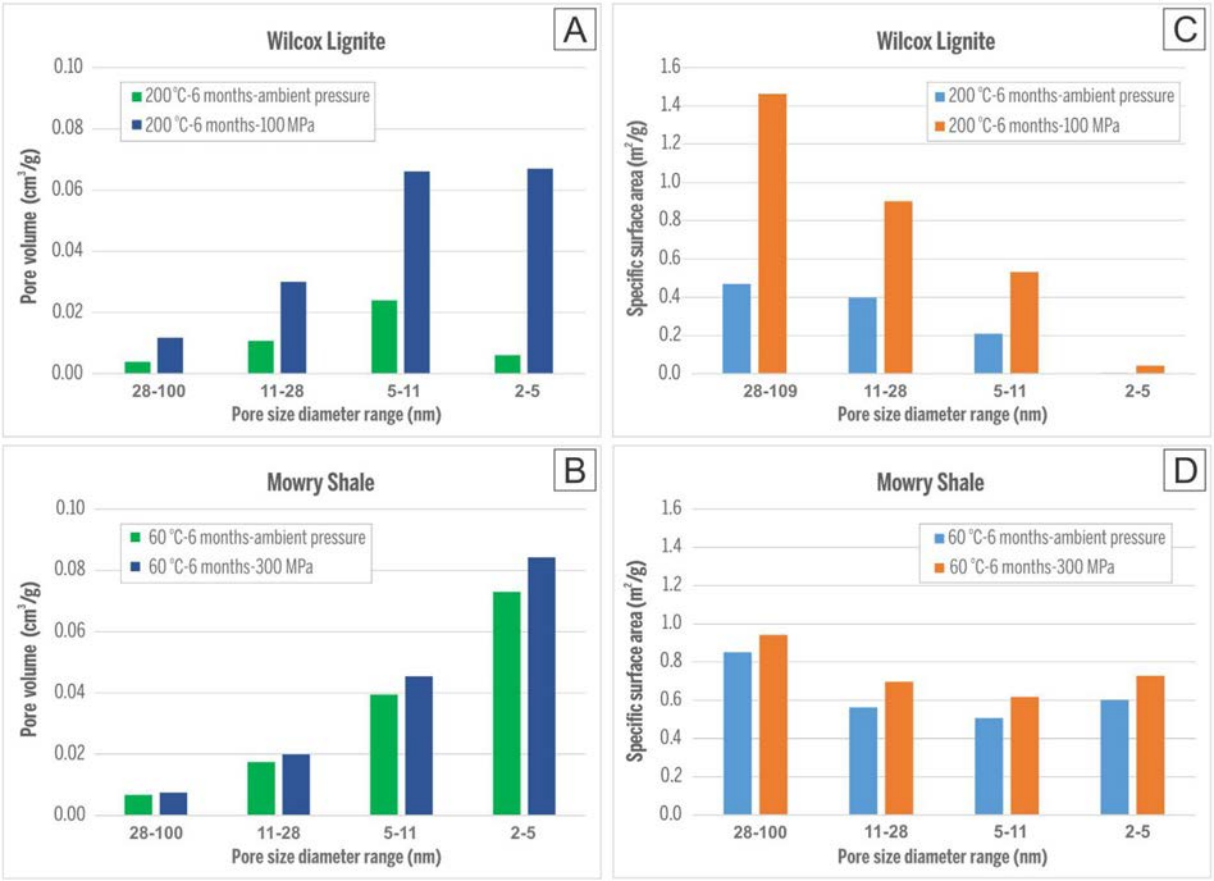

Fig. 8. Graphs showing differences in pore volumes (A, B) and specific surface areas (C, D) between ambient pressure and 100 MPa for Wilcox Coal and between ambient pressure and 300 MPa for Mowry Shale.

(Fig. 8C). This increase is much less pronounced for the shale samples, exemplified by the Mowry Shale sample (Fig. 8D).

Comparing hydrostatic conditions to experimental results using lithostatic pressure on splits of Mowry Shale and New Albany Shale at 100 MPa and 100 °C suggests that lithostatic pressure does not change micro- and mesoporosity in any significant way (Table 4, Fig. 7), probably because of the small pore sizes present in the shales studied. Of the two shales, the micro- and mesoporosities of New Albany Shale were affected more than those of Mowry Shale (Table 3), a reflection of the different original pore-size distributions and likely the different contributions of closed pores (Fig. 2A, B). Although from the values listed in Table 4 it may appear that the pressure-related changes in lithostatic conditions are more notable than those observed in hydrostatic conditions (Table 2), a direct comparison cannot be made because the samples used for experiments differ in their surface area and mesopore characteristics compared to those used earlier in hydrostatic experiments.

This experimental work and observations coming from pore size distribution are in general agreement with those documented on weakly consolidated clay rich sediments subjected to high pressures (Dewhurst et al., 1998; Day-Stirrat et al., 2012), suggesting that there is no major disconnect between the two, and that the porosimetric changes observed in our experiments are of compaction-type nature. The changes are just of a smaller magnitude because of the low original total porosity of the studied samples. As such, the results obtained can help to understand compaction related porosity modification through maturation, but their extrapolations into natural mudrock systems needs to be done with caution. The inability of experimental work to account for time-related effects such as creep, cementation, mineral dissolution, or other processes taking place during maturation, creates a difficulty to apply the results to the natural systems (Lundegard and Land, 1986; Katsube and Williamson, 1994). We note that under the conditions of our experiments, the samples have not reached the "oil window" maturity and, therefore, no effect of the fluid removal on porosimetric properties could be observed. Such effects can be prominent in higher maturity mudrocks (Wei et al., 2014).

5. Conclusions

This study results in the following conclusions:

1. Experimental temperatures of 60, 100, 200 °C and pressures of 100 MPa and 300 MPa caused only minimal changes in maturity of coal and shales over the period of 6 to 12 months.
2. The Wilcox Coal sample experienced a more pronounced temperature effect on porosity than the shale samples, suggesting that abundant organic matter pores underwent temperature-related shrinkage. Porosity changes in the shales, which had much fewer organic pores, were likely not large enough to influence overall surface areas and meso- and micropore volumes.
3. A hydrostatic pressure up to 300 MPa did not cause significant changes in the shale samples. The most notable change was an increase in mesopore volume for Wilcox Coal, likely a result of pressure-related shrinkage of macropores into mesopores.
4. A lithostatic pressure of 100 MPa did not change micro- and mesoporosities in the shale samples in any significant way. Of the two shales, the New Albany Shale was slightly more affected than Mowry Shale, likely because of the greater abundance of closed pores in the latter.

Acknowledgments

This material is based upon work supported by the U.S. Department of Energy, Office of Science, Office of Basic Energy Sciences, Chemical Sciences, Geosciences, and Biosciences Division under Award Number DE-SC0006978. Valuable comments of G. Siavalas and Ruarri Day-Stirrat greatly improved the paper.

References

Barker, C.E., Pawlewicz, M.J., 1994. Calculation of vitrinite reflectance from thermal histories and peak temperatures: a comparison of methods. In: Mukhopadhyay, P.K., Dow, W.D. (Eds.), Vitrinite Reflectance as Maturity Parameter. American Chemical Society Symposium Series, vol. 570. pp. 216–229. https://doi.org/10.1021/bk-1994-0570.ch014.

Bostick, N.H., 1973. Time as a factor in thermal metamorphism of phytoclasts (coal particles). C.r. 7. Congr. Internat. Strat. Géol. Carbonifère 2, 183–193 Krefeld.

Bustin, R.M., Rouzaud, J.N., Ross, J.V., 1995. Natural graphitization of anthracite: experimental considerations. Carbon 33, 679–691. https://doi.org/10.1016/0008-6223(94)00155-S.

Carr, A.D., 1999. A vitrinite reflectance kinetic model incorporating overpressure retardation. Mar. Pet. Geol. 16, 355–377. https://doi.org/10.1016/S0264-8172(98)00075-0.

Carr, A.D., 2000. Suppression and retardation of vitrinite reflectance, part 1. Formation and significance for hydrocarbon generation. Journal of Petroleum Geology 23, 313–343.

Clarkson, C.R., Bustin, R.M., 1996. Variation in micropore capacity and size distribution with composition in bituminous coal of the Western Canadian Sedimentary Basin: implications for coalbed methane potential. Fuel 75, 1483–1498. https://doi.org/10.1016/0016-2361(96)00142-1.

Dalla Torre, M., Ferreiro Mahlmann, R., Ernst, W.G., 1997. Geochim. Cosmochim. Acta 61, 2921–2928.

Day-Stirrat, R.J., Flemings, P.B., You, Y., Aplin, A.C., van der Pluijm, B.A., 2012. The fabric of consolidation in Gulf of Mexico mudstones. Mar. Geol. 295–298, 77–85. https://doi.org/10.1016/j.margeo.2011.12.003.

Dewhurst, D.N., Aplin, A.C., Sarda, J.-P., Yang, Y., 1998. Compaction-driven evolution of porosity and permeability in natural mudstones: an experimental study. J. Geophys. Res. 103, 651–661. https://doi.org/10.1029/97JB02540.

Gan, H., Nandi, S.P., Walker Jr., P.L., 1972. Nature of the porosity in American coals. Fuel 51, 272–277. https://doi.org/10.1016/0016-2361(72)90003-8.

Gao, L., Schimmelmann, A., Tang, Y., Mastalerz, M., 2014. Isotope rollover in shale gas observed in laboratory pyrolysis experiments: insight to the role of water in thermogenesis of mature gas. Org. Geochem. 68, 95–106. https://doi.org/10.1016/j.orggeochem.2014.01.010.

Hower, J.C., Gayer, R.A., 2002. Mechanisms of coal metamorphism: case studies from Paleozoic coalfields. Int. J. Coal Geol. 50, 215–245.

Huang, W.-L., 1996. Experimental study of vitrinite maturation: effects of temperature, time, pressure, water, and hydrogen index. Org. Geochem. 24, 233–241.

Huck, G., Patteisky, K., 1964. Inkohlungsreaktionen unter Druck. Fortschr. Geol. Rheinld. u. Westf. 12, 551–558.

Katsube, T.J., Williamson, M.A., 1994. Effects of diagenesis on shale nano-pore structure and implications for sealing capacity. Clay Miner. 29 (4), 451–472.

Kisch, H.J., Taylor, G.H., 1966. Metamorphism and alteration near an intrusive-coal contact. Economic Geology 61, 343–361.

Loucks, R.G., Reed, R.M., Ruppel, S.C., Jarvie, D.M., 2009. Morphology, genesis, and distribution of nanometer-scale pores in siliceous mudstones of the Mississippian Barnett Shale. Journal of Sedimentary Research 79, 848–861.

Lundegard, P.D., Land, L.S., 1986. Carbon dioxide and organic acids: Their role in porosity enhancement and cementation, Paleogene of the Texas Gulf Coast. In: Gautier, D.L. (Ed.), Roles of Organic Matter in Sediment Diagenesis. Society of Economic Paleontologists and Mineralogists, Special Publication 38. pp. 129–146.

Mastalerz, M., Jones, J.M., 1988. Coal rank variation in the Intrasudetic Basin, SW Poland. International Journal of Coal Geology 10, 79–97.

Mastalerz, M., Wilks, K.R., Bustin, R.M., Ross, J.V., 1993. The effect of deformation on carbonization in high-volatile bituminous and anthracitic coals. Org. Geochem. 20 (2), 315–325.

Mastalerz, M., Drobniak, A., Strąpoć, D., Solano Acosta, W., Rupp, J., 2008. Variations in pore characteristics in high volatile bituminous coals; implications for coalbed gas content. Int. J. Coal Geol. 76, 205–216. https://doi.org/10.1016/j.coal.2008.07.006.

Mastalerz, M., Drobniak, A., Schimmelmann, A., 2009. Changes in optical properties, chemistry, and micropore and mesopore characteristics of bituminous coal at the contact with dikes in the Illinois Basin. Int. J. Coal Geol. 77, 310–319. https://doi.org/10.1016/j.coal.2008.05.014.

Mastalerz, M., Schimmelmann, A., Drobniak, A., Chen, Y., 2013. Porosity of Devonian/Mississippian New Albany Shale across a maturation gradient – insights from organic petrology, gas adsorption, and mercury intrusion. AAPG Bull. 97 (10), 1621–1643. https://doi.org/10.1306/04011312194.

Milliken, K.L., Curtis, M.E., 2016. Imaging pores in sedimentary rocks: foundation of porosity prediction. Marine and Petroleum Geology 73, 590–608.

Orr, C., 1977. Pore size and volume measurement. Treatise on Analytical Chemistry (Part III) 321–358.

Price, L.C., Wenger, L.M., 1992. The influence of pressure on petroleum generation and maturation as suggested by aqueous pyrolysis. Org. Geochem. 19, 141–159.

Quaderer, A., Mastalerz, M., Schimmelmann, A., Drobniak, A., Wintsch, R.P., Bish, D.L., 2016. Dike-induced thermal alteration of the Springfield Coal (Pennsylvanian) and adjacent clastic rocks, Illinois Basin, USA. Int. J. Coal Geol. 166, 108–117. https://doi.org/10.1016/j.coal.2016.07.005.

Stadler, G., Teichmüller, R., 1971. Zusammenfassender Überblick über die Entwicklung des Bramscher Massivs und des Niedersächsischen Tektogens. Fortschr. Geol. Rheinld. U. Westf. 18, 547–564.

Taylor, G.H., 1971. Carbonaceous matter: a guide to the genesis and history of ores. Soc. Min. Geol. Japan Spec. Issue 3 (Tokyo), 283–288.

Vasseur, G., Djeran-Maigre, I., Grunberger, D., Rousset, G., Tessier, D., Velde, B., 1995. Evolution of structural and physical parameters of clays during experimental compaction. Mar. Pet. Geol. 12, 941–954. https://doi.org/10.1016/0264-8172(95)98857-2.

Wei, L., Mastalerz, M., Schimmelmann, A., Chen, L., 2014. Influence of Soxhlet-extractable bitumen and oil on porosity in thermally maturing organic-rich shales. Int. J. Coal Geol. 132, 38–50. https://doi.org/10.1016/j.coal.2014.08.003.

Wei, L., Schimmelmann, A., Mastalerz, M., Lahann, R.W., Sauer, P.E., Drobniak, A., Strąpoć, D., Mango, F.D., 2018. Catalytic generation of methane at 60 to 100oC and 0.1 to 300 MPa from source rocks containing kerogen Types I, II, and III. Geochimica et Cosmochimica Acta 231, 88–116. https://doi.org/10.1016/j.gca.2018.04.012.

Wilks, K.R., Mastalerz, M., Ross, J.V., Bustin, R.M., 1993. The effect of deformation on graphitization of anthracite. Int. J. Coal Geol. 24, 347–369.

Yang, Y., Aplin, A.C., 1998. Influence of lithology and compaction on pore size distribution and modeled permeability of some mudstones from the Norwegian margin. Mar. Pet. Geol. 15, 163–175.

Zou, Y.R., Peng, P.A., 2001. Overpressure retardation of organic-matter maturation: a kinetic model and its application. Mar. Pet. Geol. 18 (6), 707–713. https://doi.org/10.1016/S0264-8172(01)00026-5.